Vanadium, Molybdenum, and Sodium Triethanolamine Complexes Derived from an Assembly System Containing Tetrathiometalate and Triethanolamine

Yihui Chen,[†] Qiutian Liu,*[,†] Yuheng Deng,[†] Hongping Zhu,[†] Changneng Chen,[†] Hongjun Fan,[†] Daizheng Liao,[‡] and Enqing Gao[‡]

State Key Laboratory of Structural Chemistry, Fujian Institute of Research on the Structure of Matter, Chinese Academy of Sciences, Fuzhou, Fujian 350002, China, and Department of Chemistry, Nankai University, Tianjing 300071, China

Received January 30, 2001

The reaction system composed of triethanolamine (TEA) and tetrathiovanadate in the presence of MeONa (MeOLi) or $NaNH_2$ was studied to afford vanadium and alkali metal TEA complexes. Complexes $\{M\subset V_6O_6[N(CH_2CH_2O)_2(CH_2CH_2OH)]_6\}_2S_6$ (M = Na (**1**), Li (**2**)) contain two cyclic $V^{(IV)}$ [12]metallacrown-6 cations linked by a polysulfide S_6^{2-} anion. Also separated from the reaction system is a novel sodium TEA complex $\{[Na(TEA)]_2S_6\}_n$ (**3**), in which parallel coordination chains $[Na(TEA)^+]_n$ are connected by O−H···S hydrogen bonds forming 3-D network structure. Variable-temperature conductance of **3** was determined to display semiconductor feature. The desulfurization of VS_4^{3-} was observed to form S_6^{2-} anion and/or S_8 molecule in the synthetic reactions of **1**−**3**. A striking contrast was noted that MoS_4^{2-} did not desulfurize in the similar reaction to that of VS_4^{3-} with TEA, and a Na/TEA complex containing MoS_4^{2-}, $(Et_4N)_2[Na_2(\mu\text{-TEA})_2(CH_3OH)_2](MoS_4)_2$ (**4**), was obtained instead. The S···H−O and O···H−O hydrogen bonds play an important role in forming the one- or three-dimensional structures for all these complexes by the linkages between clusters and chains. The IR spectrum indicates the structural similarity of complexes **1** and **2**. For complex **4**, the Mo═S stretch vibration at 468 cm^{-1} showing widening and slight red-shift and the slight movement of the ^1H NMR signals of TEA ligand to downfield are considered to be the influence of the S···H−O hydrogen bonds. Variable temperature magnetic susceptibility data were collected for complex **1**. The effect magnetic moment per V_6 unit varies gradually from 4.04 μ_B at 300 K to 6.24 μ_B at 5 K, exhibiting ferromagnetic interaction. Heisenberg-type vector-coupling model and molecular field approximation were used to treat the interaction between the paramagnetic sites and gave a good fitting result: $J = 3.97$ cm^{-1}, $J' = 1.99$ cm^{-1}, $g = 1.99$, $F = 3.64 \times 10^{-3}$. Density functional calculation was also performed to complex **1** and its Li, K analogues. The lowest total bonding energy of −874.001 eV was obtained for $[Na\subset V_6(\mu_3\text{-O})_6]$ complex containing six unpaired electrons, indicating the stability of a V_6 system with six independent spins $S = {}^1/_2$. When the alkali metal ion is inserted into the $[V_6(\mu_3\text{-O})_6]$ cavity, the positive values of the bonding interaction (E_b) indicate that the insertion depresses the total energy and that complexes **1** and **2** together with K^+ complex may exist. However, the lowest E_b value of the K^+ complex implies its instability.

Introduction

Triethanolamine (TEA) has attracted increased interest[1] in metal coordination chemistry. Metal triethanolamine complexes have covered most of the metals of period table including the elements in groups 1,[2] 2,[2a,3] 3,[4] 4[5] and 5,[6] transition elements,[5c,7−19] and lanthanides[20] for the multifarious purposes, such as biological activities of enzymes,[15] supramolecular chemistry,[14] and low-temperature MOCVD techniques[21] etc. Although TEA as a tetradentate ligand has been extensively used to prepare mononuclear metal complexes with a variety of monomeric tricyclic structures (metalatrane), its ability as a coordinating ligand to synthesize polynuclear metal complexes has not been extensively investigated. So far, the polynuclear metal TEA complexes reported contain a few structure types such as dimeric metalatranes for Ba[2a] and Ti,[7,12,19] trimeric metalatrane for Sn,[5b] tetranuclear complex for Al,[4] metallacrown ether for Fe,[14] and

* To whom correspondence should be addressed.
[†] Chinese Academy of Sciences.
[‡] Nankai University.

(1) Verkade, J. G. *Acc. Chem. Res*. **1993**, *26*, 483−489.
(2) (a) Naiini, A.; Pinkas, J.; Plass, W.; Young, V. G., Jr.; Verkade, J. G. *Inorg. Chem*. **1994**, *33*, 2137. (b) Voegel, J. C.; Fischer, J.; Weiss, R. *Acta Crystallogr*. **1974**, *B30*, 62. (c) Padmanabhan, V. M.; Jakkal, V. S.; Poonia, N. S. *Acta Crystallogr*. **1987**, *C43*, 1061−1064.
(3) (a) Naiini, A.; Young, V. G., Jr.; Verkade, J. G. *Polyhedron* **1997**, *16*, 2087. (b) Poncelet, O.; Hubert-Pfalzgraf, L. G.; Toupet, L. *Polyhedron* **1991**, *10*, 2045−2050. (c) Hundal, G.; Martinez-Ripoll, M.; Hundal, M. S.; Poonia, N. S. *Acta Crystallogr*. **1996**, *C52*, 789−792. (d) Hundal, G.; Martínez-Ripoll, M. *Acta Crystallogr*. **1996**, *C51*, 1788−1791.
(4) Healy, M. D.; Barrom, A. R. *J. Am. Chem. Soc*. **1989**, *111*, 398−399.
(5) (a) Sienkiewicz, A. V.; Kokozay, V. N. *Polyhedron* **1994**, *13*, 1431−1437. (b) Swisher, R. G.; Day, R. O.; Holmes, R. R. *Inorg. Chem*. **1983**, *22*, 3692−3695. (c) Naiini, A. A.; Young, V.; Verkade, J. G. *Polyhedron* **1995**, *14*, 393−400. (d) Narula, S. P.; Soni, S.; Shankar, R.; Chadha, R. K. *J. Chem. Soc., Dalton* Trans. **1992**, 3055−3056. (e) Narula, S. P.; Shanker, R.; Kumar, M.; Chadha, R. K.; Janaik, C. *Inorg. Chem*. **1997**, *36*, 1268−1273. (f) Sienkiewicz, A. V.; Kokozay, V. N. *Polyhedron* **1994**, *13*, 1431−1437.
(6) Clardy, J. C.; Milbrath, D. S.; Springer, J. P.; Verkade, J. G. *J. Am. Chem. Soc*. **1975**, *97*, 623−624.
(7) Menge, W. M. P. B.; Verkade, J. G. *Inorg. Chem*. **1991**, *30*, 4628−4631.
(8) Wieghardt, K.; Kleine-Boymann, M. *J. Chem. Soc., Dalton Trans*. **1985**, 2493−2497.
(9) Boche, G.; Möbus, K.; Harms, K.; Marsch, M. *J. Am. Chem. Soc*. **1996**, *118*, 2770−2771.
(10) Nugent, W. A.; Harlow, R. L. *J. Am. Chem. Soc*. **1994**, *116*, 6142−6148.

10.1021/ic010126c CCC: $20.00
Published on Web 06/19/2001

extented structure for alkali metal complexes.[2a] It is worthwhile to notice that in the alkali and alkali earth metal TEA complexes hydrogen bonding interactions play an important role in forming unlimited network structure. We have briefly reported a sodium TEA complex $\{[NaN(CH_2CH_2OH)_3]_2S_6\}_n$[22] which contains unlimited coordination chains $[Na(TEA)^+]_n$ together with a S_6^{2-} linkage forming a 3-D network by O−H···S hydrogen bonds. The sodium TEA complex was obtained in an assembly system of $(NH_4)_3VS_4$/TEA/$NaNH_2$ and became the first example containing the O−H···S hydrogen bond in the crystal structure for the metal TEA complexes. In the further study on the reaction system containing tetrathiometalate and TEA, we have obtained V/Na and Mo/Na TEA complexes, exhibiting obvious difference between the V and Mo chemistry. Herein we describe the synthesis, structure, and magnetic property of the first polynuclear V/TEA complex $\{Na\subset V_6O_6[N(CH_2CH_2O)_2(CH_2CH_2OH)]_6\}_2S_6$. The density functional calculation of the complex for explanation of the structure is also performed. Meanwhile, the molybdenum and sodium TEA complexes obtained from the reaction system studied are also reported.

Experimental Section

All operations were carried out under dinitrogen atmosphere using Schlenk techniques. The solvents were dried with molecular sieves and degassed prior to use. Reagents TEA, NaOMe, LiOMe, $NaNH_2$, and Et_4NCl are commercially available without further purification. Compounds $(NH_4)_3VS_4$[23] and $(NH_4)_2MoS_4$[24] were obtained by literature method.

$\{Na\subset V_6O_6[N(CH_2CH_2O)_2(CH_2CH_2OH)]_6\}_2S_6\cdot 2CH_3OH$ (1·2CH$_3$OH). A solution of 0.46 g of $(NH_4)_3VS_4$ (2 mmol) in 25 mL of MeOH was treated with 0.45 g (3 mmol) of TEA and 0.33 g (6.1 mmol) of NaOMe, and the solution was stirred for 48 h at room temperature. After filtration, the green filtrate was concentrated in vacuo to remove 12 mL of MeOH. The solution was allowed to stand for several days. Green prismy crystals deposited were filtered and dried in vacuo, affording 0.1 g (yield, 21%) of **1**·2CH$_3$OH. Anal. Calcd for $C_{72}H_{156}N_{12}Na_2O_{48}S_6V_{12}\cdot 2CH_3OH$: C, 30.95; H, 5.76; N, 5.85; S, 6.70. Found: C, 31.30; H, 5.26; N, 5.74; S, 6.75. IR (KBr, cm^{-1}): 462 (V−O$_b$), 544 (S−S), 958 (V═O), 1087 (C−O), 1463 (C−N), 3382 (O−H).

$\{Li\subset V_6O_6[N(CH_2CH_2O)_2(CH_2CH_2OH)]_6\}_2S_6$ (2). This compound was obtained by the same procedure as in the preceding preparation with the use of 0.23 g (6.1 mmol) of LiOMe instead of NaOMe. Green crystals (0.08 g, yield 17%) of **2** was obtained. Anal. Calcd for $C_{72}H_{156}Li_2N_{12}O_{48}S_6V_{12}$: C, 31.15; H, 5.67; N, 6.06. Found: C, 31.14; H, 5.70; N, 6.28. IR (KBr, cm^{-1}): 461 (V−O), 548 (S−S), 949 (V═O), 1090 (C−O), 1469 (C−N), 3390 (O−H).

$\{[NaN(CH_2CH_2OH)_3]_2S_6\}_n$ (3). To 1.12 g of TEA (7.5 mmol) in 25 mL of CH_3OH, 0.23 g of $(NH_4)_3VS_4$ (1 mmol) was added in the presence of 0.12 g (3.1 mmol) of $NaNH_2$. The solution was stirred for 48 h at room temperature and then it was filtered. The wine-red filtrate was concentrated in vacuo to remove 12 mL of CH_3OH and was allowed to stand for several days at 5 °C, affording orange-red prism crystals which were filtered and dried in vacuo to yield 0.14 g (yield 39.3%) of **3**. Anal. Calcd for $C_{12}H_{30}N_2Na_2O_6S_6$: C, 26.85; H, 5.63; N, 5.22; S, 35.98. Found: C, 27.47; H, 5.61; N, 5.32; S, 36.36. IR (KBr, cm^{-1}): 545 (S−S), 1068 (C−O), 1446 (C−N), 3154 (O−H). ^{1}H NMR (DMSO-d_6, ppm): δ 4.36 (OH), 3.40 (OCH_2), 2.54 (NCH_2). ^{13}C NMR (DMSO-d_6, ppm): δ 57.47, 59.54.

$(Et_4N)_2[Na_2(\mu\text{-}TEA)_2(CH_3OH)_2](MoS_4)_2$ (4). A solution of 0.52 g of $(NH_4)_2MoS_4$ (2 mmol) in 30 mL of MeOH was treated with 1.12 g of TEA (7.5 mmol), 0.12 g (2.5 mmol) of $NaNH_2$, and 0.66 g (4 mmol) of Et_4NCl. The solution was stirred for 16 h at room temperature. After filtration, the red filtrate was allowed to stand for 3 days at room temperature. The microcrystals deposited were filtered out and the resultant solution was stored at refrigerator for 30 days to afford 0.82 g (yield 73.4%) of red rectangular crystals of **4**. Anal. Calc. for $C_{30}H_{78}Mo_2N_4Na_2O_8S_8$: C, 32.25; H, 7.03; N, 5.01. Found: C, 32.78; H, 6.65; N, 5.84. IR (KBr, cm^{-1}): 468 (Mo═S), 1065 (C−O), 1457 (C−N), 3300 (O−H). ^{1}H NMR (DMSO-d_6, ppm): δ 1.25 (CH_3, Et_4N^+), 2.76 (NCH_2, TEA), 3.28 (CH_2, Et_4N^+), 3.69 (OCH_2, TEA), 4.81 (OH, TEA).

X-ray Structure Determination. $\{Na\subset V_6O_6[N(CH_2CH_2O)_2(CH_2CH_2OH)]_6\}_2S_6\cdot 2CH_3OH$ (1·2CH$_3$OH). A clear green prismy crystal (0.55 × 0.40 × 0.30 mm) was selected and was coated with epoxy resin and mounted on a glass fiber for X-ray data collection. Intensity data were collected on an Enraf Nonius CAD4 diffractometer using Mo Kα (λ = 0.71073 Å) radiation and ω-2θ scan mode with the maximum 2θ of 52°. The unit cell constants were determined from a least-squares fit of the setting angles for 25 reflections (14° < θ < 15°). The intensities of three standard reflections were examined and 5.8% decay was found at the end of the collection. Lorentz-polarization and empirical absorption correction were applied. A total of 8194 unique reflections were observed with $I > 3\sigma(I)$ and were used in calculations.

The structure was solved by direct methods and subsequent difference Fourier syntheses using the MolEN/PC program.[25] Hydrogen atoms were geometrically located and added to the structure factor calculations but their positions were not refined. All non-hydrogen atoms were refined with anisotropic thermal parameters. There are three oxygen atoms, O14, O17, and O26, to be disordered in two positions, respectively, with the occupancies of 0.5 for each of them. A S_6^{2-} anion was found in the structure to link two [12]vanadiumcrown-6 units, all the S atoms in the anion were disordered in two positions relative to a symmetrical site as shown in Figure 1. The final refinement included 760 variable parameters and converged to $R = 0.0487$ and $R_w = 0.0691$

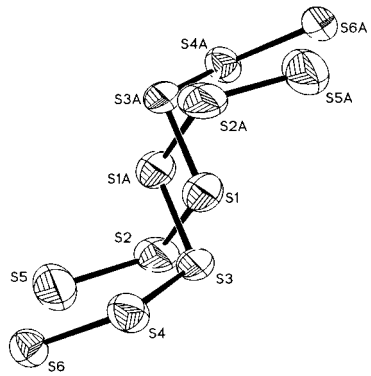

Figure 1. Structure of the S_6^{2-} anion in complex **1**. Each S atom is disordered at both positions with the occupancy of 0.5.

(11) Ramalingam, K.; Aravamudan, G.; Seshasayee, M. *Z. Kristallogr.* **1987**, *181*, 215−222.
(12) Naiina, A. A.; Ringrose, S. L.; Su, Y.; Jacobson, R. A.; Verkade, J. G. *Inorg. Chem.* **1993**, *32*, 1290−1296.
(13) Pinkas, J.; Huffman, J. C.; Bollinger, J. C.; Streib, W. E.; Baxter, D. V.; Chisholm, M. H.; Cauton, K. G. *Inorg. Chem.* **1997**, *36*, 2930−2937.
(14) Saalfrank, R. W.; Bernt, I.; Uller, E.; Hampel, F. *Angew. Chem., Int. Ed. Engl.* **1997**, *36*, 2482−2485.
(15) Crans, D. C.; Chen, H.; Anderson, O. P.; Miller, M. M. *J. Am. Chem. Soc.* **1993**, *115*, 6769−6776.
(16) Kitagawa, S.; Munakata, M.; Ueda, M. *Inorg. Chim. Acta* **1989**, *164*, 49−53.
(17) Kapteijn, G. M.; Baesjou, P. J.; Alsters, P. L.; Grove, D. M.; Smeets, W. J. J.; Kooijman, H.; Spek, A. L.; van Koten, G. *Chem. Ber.* **1997**, *130*, 35−44.
(18) Zhou, Y.-Z.; Jin, X.-L.; Liu, S.-C. *J. Chin. Struct. Chem.* **1993**, *12*, 48−51.
(19) Naiini, A. A.; Menge, W. M. P. B.; Verkade, J. G. *Inorg. Chem.* **1991**, *30*, 5009−5012.
(20) (a) Kessler, V. G.; Hubert-Pfalzgraf, L. G.; Halut, S.; Daran, J. C. *J. Chem. Soc., Chem. Commun.* **1994**, 705−706. (b) Hahn, F. E.; Mohr, J. *Chem. Ber.* **1990**, *123*, 481−484.
(21) Chi, K. M.; Shin, H. K.; Hampden-Smith, M. J.; Duesler, E. N.; Kodas, T. T. *Polyhedron* **1991**, *10*, 2293.
(22) Chen, Y.; Zhu, H.; Liu, Q.; Chen, C. *Chem. Lett.* **1999**, 585−586.
(23) Do, Y.; Simhon, E. D.; Holm, R. H. *Inorg. Chem.* **1985**, *24*, 4635.
(24) McDonald, J. W.; Friesen, G. D.; Rosenhein, L. D.; Newton, W. E. *Inorg. Chim. Acta* **1981**, *72*, 205.
(25) *MolEN, An Interactive Structure Solution Procedure*; Enraf-Nonius: Delft, The Netherlands, 1990.

Table 1. Crystallographic Data for Compounds **1**, **3**, and **4**

	1	**3**	**4**
empirical formula	$C_{74}H_{164}N_{12}Na_2O_{50}S_6V_{12}$	$C_{12}H_{28}N_2Na_2O_6S_6$	$C_{30}H_{78}Mo_2N_4Na_2O_8S_8$
fw	2871.85	534.73	1117.35
λ(Mo Kα)	0.71073	0.71073	0.71069
T, °C	20	20	20
space group	$P\bar{1}$ (No. 2)	$C2/c$	$P\bar{1}$ (No. 2)
a, Å	14.374(3)	22.5075(5)	9.098(8)
b, Å	14.486(3)	7.2826(21)	9.715(8)
c, Å	15.152(3)	16.4646(28)	14.909(5)
α, deg	73.94(2)		106.54(5)
β, deg	80.29(2)	119.961(11)	90.11(6)
γ, deg	72.75(2)		94.76(6)
V, Å^3	2882.4(1)	2338.1(3)	1258(3)
Z	1	4	1
ρ_{calcd}, g/cm^3	1.62	1.52	1.47
μ, mm^{-1}	1.09	0.63	0.86
R[a]	0.0487	0.0368	0.0386
R_w[b]	0.0691	0.0425	0.0696

[a] $R = \sum||F_o| - |F_c||/\sum|F_o|$. [b] $R_w = [\sum w(|F_o| - |F_c|)^2/\sum wF_o^2]^{1/2}$. **1**, **3**: $w = 1/[S^2(F)]$. **4**: $w = 1/[S^2(F) + (0.030F)^2 + 1.0] - F$.

with $(\Delta/\sigma)_{max} = 0.0094$, $(\Delta\rho)_{max} = 1.42$ e Å^{-3}, and $(\Delta\rho)_{min} = -0.09$ e Å^{-3}. The imbalance between the largest difference peak and hole comes from the disordered treatment of the sulfur atoms in counteranion S_6^{2-}, which is necessary for the solution of the structure.

{[NaN(CH$_2$CH$_2$OH)$_3$]$_2$S$_6$}$_n$ (3). Structure determinations of complex **3** and the following complex **4** are similar to that of complex **1**, and experimental details are only provided if different from that used for complex **1**. An orange-yellow prismy crystal (0.06 × 0.04 × 0.01 mm) was used for X-ray data collection. The unit cell constants were determined from 25 reflections ($11° < \theta < 15°$). The intensities of three standard reflections were examined and 5.2% decay was found. A total of 2445 unique reflections were observed with $I > 3\sigma(I)$ and were used in calculations.

The final refinement included 183 variable parameters and converged to $R = 0.0368$ and $R_w = 0.0425$ with $(\Delta/\sigma)_{max} = 0.0005$, $(\Delta\rho)_{max} = 0.18$ e Å^{-3}, and $(\Delta\rho)_{min} = -0.03$ e Å^{-3}.

(Et$_4$N)$_2$[Na$_2$(μ-TEA)$_2$(CH$_3$OH)$_2$](MoS$_4$)$_2$ (4). A dark red rectangular crystal (1.50 × 0.60 × 0.40 mm) was used for X-ray data collection on an AFC5R Rigaku diffractometer using Mo Kα ($\lambda = 0.71069$ Å) radiation. The unit cell constants were determined from 20 reflections ($15° < \theta < 20°$). The intensities of three standard reflections were examined and the maxmum decay of 20% was found. A total of 4247 unique reflections were observed with $I > 3\sigma(I)$ and were used in calculations.

The final refinement included 260 variable parameters and converged to $R = 0.0386$ and $R_w = 0.0696$ with $(\Delta/\sigma)_{max} = 0.0133$, $(\Delta\rho)_{max} = 0.93$ e Å^{-3}, and $(\Delta\rho)_{min} = -0.16$ e Å^{-3}.

The crystallographic data for **1**, **3**, and **4** are listed in Table 1.

Other Physical Measurements. The IR spectra were recorded on a Bio-Rad FTS-40 Model spectrophotometer. The ^{1}H NMR spectrum was recorded on a Bruker-Am 500 spectrometer with TMS as standard. The variable temperature susceptibilities were measured on a Model CF-1 superconducting extraction sample magnetometer with crystalline sample kept in capsule at 5∼300 K. The susceptibilities were corrected for diamagnetism of the constituent atoms using Pascal′ constants for compound **1**.

Results and Discussion

Structural Features. {Na⊂V$_6$O$_6$[N(CH$_2$CH$_2$O)$_2$(CH$_2$CH$_2$OH)]$_6$}$_2$S$_6$·2CH$_3$OH. Compound **1** is the first example of hexanuclear vanadium TEA complex. Its cell unit contains a crystallographically independent molecule {Na⊂V$_6$O$_6$[N(CH$_2$CH$_2$O)$_2$(CH$_2$CH$_2$OH)]$_6$}$_2$S$_6$·2CH$_3$OH consisting of two cyclic V$^{(IV)}$ [12]metallacrown-6 structural units {Na⊂V$_6$O$_6$[N(CH$_2$CH$_2$O)$_2$(CH$_2$CH$_2$OH)]$_6$}$^+$ (Figure 2), in which a sodium ion is encapsulated in the center of hexagonal cluster. The six V atoms are alternately divided into two sets of parallel V_3 planes and distribute above and below the least-squares plane by ±0.127 Å in which the Na^+ ion locates, forming a centrosymmetric V_3/Na/V_3 structure. The dihedral angle of 118.8° was found between the least-squares planes of the two V_6 units. Counterion S_6^{2-} exists between the two cations and connects them by S···H—O hydrogen bonds as shown in Figure 3. Similar [12]-metallacrown-6 is {Na⊂Fe$_6$[N(CH$_2$CH$_2$O)$_3$]$_6$}$^+$,[14] which almost resembles the [12]vanadylacrown-6 analogue in shape and in the metal coordination sphere, except for a V═O bond and a free CH$_2$CH$_2$OH arm existing in the latter (vide infra). The separations between two neighboring V atoms range from 3.2632(1) Å to 3.2868(1) Å, and the V···Na separations have average value of 3.269 Å, exhibiting no metal—metal bonding interaction. The interior angles of the V_6 hexagon are near to 120°; the distance between two opposite vanadium atoms of the hexagon is 6.514 Å. The distorted octahedral coordination sphere of the V atoms is composed of one N atom and two μ_2- and μ_3-O atoms of TEA ligands. In addition, one oxo donor coordinates to the V atom to form a V═O double bond (mean 1.608(10) Å) which makes obvious difference between the V and the Fe crown ethers. It is also noted that there is one set of free CH$_2$CH$_2$OH arm of TEA existing out of the coordination sphere in the V crown ether different from the Fe one. Consequently, six VO[N(CH$_2$CH$_2$O)$_2$(CH$_2$CH$_2$OH)] subunits

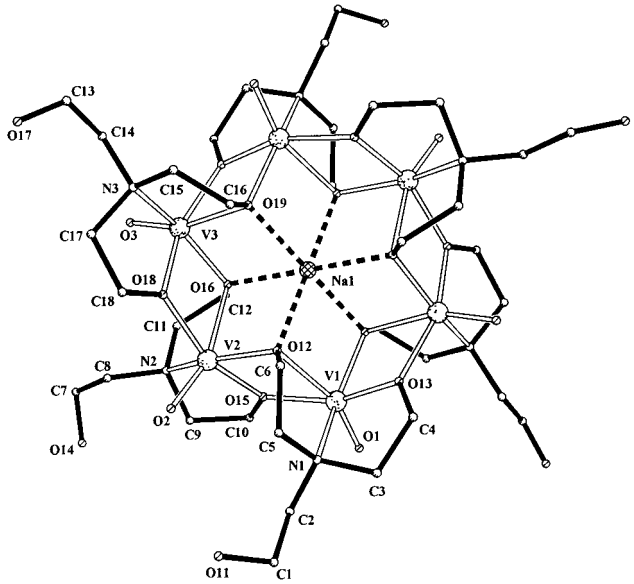

Figure 2. ORTEP diagram of the cyclic V$_6^{(IV)}$ [12]metallacrown-6 cation.

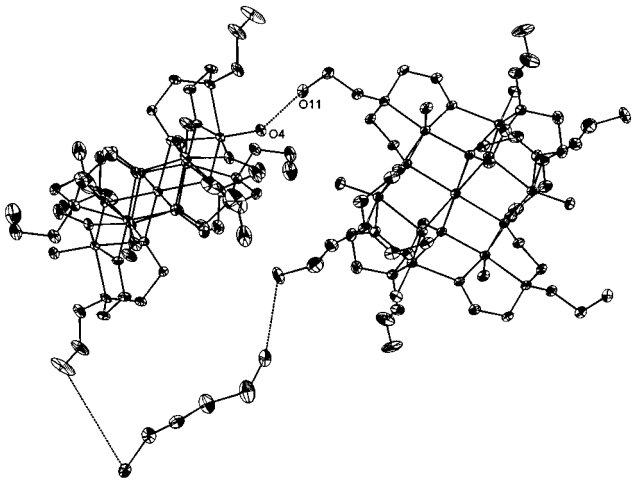

Figure 3. Molecular structure of complex **1**, showing two [12]-metalacrown-6 cations connected by S_6^{2-} anion. The S···H−O hydrogen bonds are listed as follows: S6···O14A, 3.29 Å; S4···O14A, 3.69 Å; S5A···O23, 2.75 Å; S6A···O23, 3.70 Å

connect each other by two μ_2-oxygen atoms of the deprotonized hydroxyl groups of TEA to form the structure of the V crown ethyl. The distance (mean 2.205 Å) of V−μ_3O bond opposite to V=O is obviously longer than those of other V−O bonds with mean distance of 1.995 Å, exhibiting the strong trans-effect of the oxo donor. Selected bond distances and angles are listed in Table 2 for one V_6 cation only and the S_6^{2-} anion since the structural parameters are very close between the two cluster cations.

The sodium ion locating in the center of the cation forms a coordination sphere from the six μ_3-O atoms with distorted octahedron configuration. The mean Na−O bond distance is 2.303 Å and the separations between opposite μ_3-O atoms range from 4.55 to 4.69 Å, meaning that the size of μ_3-O_6 cavity just corresponds the sum (2.33 Å) of the ionic radius of O^{2-} and Na^+.

The presence of the CH_2CH_2OH groups makes extensive hydrogen bonding interactions with the V=O group and the S_6^{2-} anion in the lattice as shown in Figure 4. The O−H···S and O−H···O hydrogen bonds closely connect the two V_6 components. For example, O11···O14 (2.78 Å) links the CH_2-CH_2OH and V=O groups, while O14A and O23 link both sides of the S_6^{2-} anion (Figure 3), respectively. Because of disordered distribution of these oxygen and sulfur atoms, their hydrogen bonding interactions exhibit more complicated features. The O−H···S hydrogen bonds range from 2.75 to 3.70 Å. In addition to form the hydrogen bonds existing between both V_6 components, each S_6^{2-} anion also links other hydroxyls, correlating the molecules between obvious layers. Also the oxygen atom in vanadyl group forms the hydrogen bonds between the layers with the free CH_2CH_2OH arms. These hydrogen bond interactions between the molecule layers lead to the formation of a complicated three-dimensional hydrogen bonding polymers as shown in Figure 4.

$\{[NaN(CH_2CH_2OH)_3]_2S_6\}_n$ (3). The structure of **3** contains a $[Na(TEA)^+]_n$ chain with positive charges and S_6^{2-} anions as shown in Figure 5. Among the three CH_2CH_2OH arms of TEA two hydroxyl groups are bridged to two Na ions forming double μ-OH bridges and an unlimited $Na_2(\mu\text{-OH})_2$ zigzag chain. All the zigzag chains are parallel to each other. Distorted octahedral sodium ion is coordinated by five oxygen atoms and a nitrogen atom from three TEA molecules. Related bond distances and angles are listed in Table 3. The Na−O_{chain} distances ranging from 2.419(1) Å to 2.481(2) Å are obviously longer than other Na−O distance of 2.384(2) Å, since the OH group in the zigzag chain shares its electron density between both Na−O bonds, lengthening the Na−O_{chain} distance. No significant hydrogen bond was found between these hydroxyl groups, the shortest O···O distance (O3A···O2) was observed to be 3.016 Å. Both ends of the S_6^{2-} anion are linked to the parallel $[Na(TEA)]_n$ chains by O−H···S hydrogen bonds ranging from 3.17 Å to 3.21 Å to form three-dimensional network structure as shown in Figure 6. Two kinds of inner cavities in the structure were found. The size of the big cavity enclosed by 30 atoms was marked by opposite S atoms and O atoms, respectively, to be S···S 12.85 Å and O···O 9.14 Å. The small cavity is composed of 12 atoms including 4OH, 2Na, and 2S with dimensions of 8.8 Å (Na···Na) and 7.8 Å (O···O).

$(Et_4N)_2[Na_2(\mu\text{-TEA})_2(CH_3OH)_2](MoS_4)_2$ (4). Similar to the metalatrane[2a,7,12] compound **4** also contains the metalatrane $[Na(TEA)]^+$ subunit and shows its dimeric metalatrane structure as presented in Figure 7. A crystallographically imposed symmetrical center locates in the center of the $Na_2(\mu\text{-O})_2$ moiety.

Table 2. Selected Bond Distances (Å) and Angles (deg) of Compound **1**

V1···V2	3.2817(1)	V2···V3	3.2868(1)
V1···V3A[a]	3.2632(1)	S1−S2	2.0255(5)
S1−S3A	2.0531(4)	S2−S5	2.0060(7)
S3A−S4A	2.0536(5)	S4A−S6A	2.0303(5)
V1−O1	1.612(4)	V1−O13	1.952(3)
V1−O15	2.036(3)	V1−O12	2.210(3)
V1−O19A[a]	1.998(3)	V1−N1	2.206(4)
V2−O2	1.602(4)	V2−O15	1.945(4)
V2−O16	2.219(4)	V2−O18	2.043(3)
V2−O12	1.995(3)	V2−N2	2.199(4)
V3−O3	1.616(3)	V3−O13A[a]	2.034(3)[a]
V3−O16	1.995(3)	V3−O18	1.945(4)
V3−O19	2.173(3)	V3−N3	2.208(5)
Na1−O12	2.277(3)	Na1−O16	2.345(2)
Na1−O19	2.298(3)		
O1−V1−O13	105.1(1)	O3−V3−O16	105.9(2)
O1−V1−O15	95.3(1)	O18−V3−O19	90.2(2)
O1−V1−O12	160.7(1)	O18−V3−N3	80.1(1)
O1−V1−O19A[a]	105.5(2)	O19−V3−N3	77.1(1)
O1−V1−N1	94.4(2)	O3−V3−O18	105.5(2)
O12−V1−O13	90.9(1)	O3−V3−O19	160.6(1)
O12−V1−O15	69.8(1)	O3−V3−N3	94.3(2)
O12−V1−O19A[a]	88.5(1)	O16−V3−O18	76.7(1)
O12−V1−N1	77.4(1)	O16−V3−O19	88.4(1)
O13−V1−O15	159.3(1)	O16−V3−N3	152.5(1)
O13−V1−O19A[a]	76.2(1)	O3−V3−O13A[a]	94.5(2)
O13−V1−N1	80.5(1)	O13A[a]−V3−O16	95.4(1)
O15−V1−N1	101.5(1)	O13A[a]−V3−O18	159.7(1)
O15−V1−O19A[a]	95.4(1)	O13A[a]−V3−O19	70.7(1)
O19A[a]−V1−N1	152.5(1)	O13A[a]−V3−N3	101.5(1)
O2−V2−O15	106.2(2)	O16−Na1−O19	77.5(1)
O2−V2−O16	160.6(1)	O19−Na1−O19A[a]	180.0(9)
O2−V2−O18	95.4(2)	O16−Na1−O19A[a]	102.5(1)
O2−V2−N2	93.5(2)	O12−Na1−O19	100.0(1)
O2−V2−O12	104.6(1)	O12−Na1−O19A[a]	80.0(1)
O12−V2−O15	76.2(1)	O16−Na1−O19	77.5(2)
O12−V2−O16	90.1(1)	O12−Na1−O16	80.44(9)
O12−V2−O18	97.4(1)	O12−Na1−O12A[a]	180.0(7)
O12−V2−N2	153.4(2)	O16−Na1−O16A[a]	180.0(7)
O15−V2−O18	158.4(1)	V1−O12−V2	102.5(1)
O15−V2−N2	80.1(1)	V1−O13−V3A[a]	109.9(1)
O15−V2−O16	89.3(1)	V1−O15−V2	111.0(1)
O16−V2−O18	69.9(1)	V2−O16−V3	102.4(2)
O16−V2−N2	77.5(1)	V1A[a]−O19−V3	102.9(1)
O18−V2−N2	100.1(1)	V2−O18−V3	111.0(2)
S1−S2−S5	109.7(2)	S1−S3A−S4A	108.6(2)
S2−S1−S3A	109.1(2)	S3A−S4A−S6A	108.7(2)

[a] Symmetrical operation: $2 - x, 2 - y, -z$.

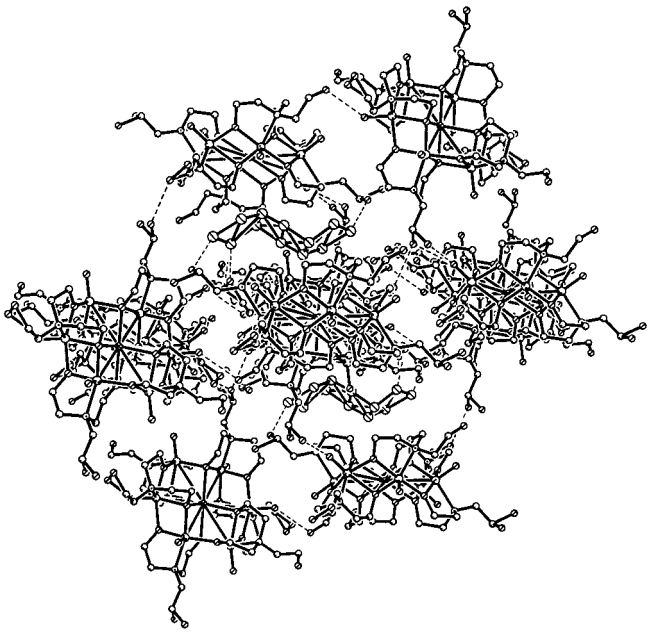

Figure 4. Stereoview of the packing of $\{Na\subset V_6O_6[N(CH_2CH_2O)_2(CH_2CH_2OH)]_6\}_2S_6$. The hydrogen bonds were drawn in dotted line.

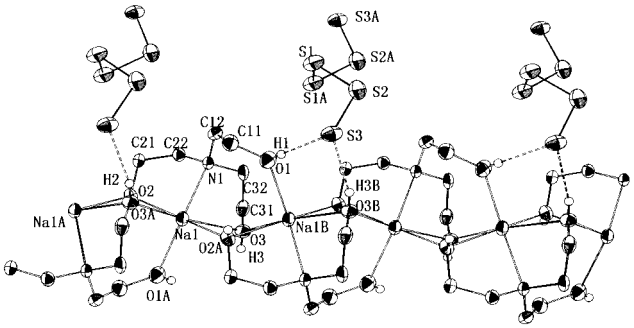

Figure 5. ORTEP representation of $\{[NaN(CH_2CH_2OH)_3]_2S_6\}_n$ with thermal ellipsoids at 50% probability. The hydrogen bonds were drawn in dotted line. All H atoms in CH_2 groups are omitted.

Table 3. Selected Bond Distances (Å) and Angles (deg) for Compound **3**

S1−S1A	2.059(1)	S1−S2	2.0336(9)
S2−S3	2.0428(8)	Na1−O1	2.384(2)
Na1−O2	2.453(2)	Na1−O2A	2.419(1)
Na1−O3	2.481(2)	Na1−O3A	2.426(2)
Na1−N1	2.573(2)		
S1−AS1−S2	107.10(5)	S1−S2−S3	109.06(4)
O1A−Na1−O2	84.79(6)	O1A−Na1−O2A	98.28(6)
O1A−Na1−O3	90.12(6)	O1A−Na1−O3A	98.32(6)
O1A−Na1−N1	139.55(6)	O2−Na1−O2A	168.84(7)
O2−Na1−O3	114.88(5)	O2−Na1−O3A	76.35(5)
O2−Na1−N1	73.04(5)	O2A−Na1−O3	75.96(5)
O2A−Na1−O3A	92.56(5)	O2A−Na1−N1	110.03(6)
O3−Na1−O3A	166.68(6)	O3−Na1−N1	70.35(6)
O3A−Na1−N1	108.32(7)	Na1−O2−Na1A	97.46(4)
Na1−O3A−Na1A	96.52(6)		

The six-coordinate sodium ion is bonded to the four heteroatoms of a TEA molecule, the oxygen of a methanol, and the oxygen of an OH group from a neighboring subunit. The structure of **4** differs from that of other dimer metalatrane analogues in this respect, wherein MoS_4^{2-} anion links the metalatrane $[Na(TEA)]^+$ subunit to form a dimeric structural unit $\{[Na(\mu\text{-}TEA)(CH_3OH)(MoS_4)]_2\}^{2-}$ (Figure 7) by five S···H−O hydrogen bonds as follows: S4···O1A, 3.36 Å; S2···O2, 3.43 Å; S1···O3, 3.45 Å; S1···O2, 3.40 Å; S4···O3, 3.42 Å. In addition, the

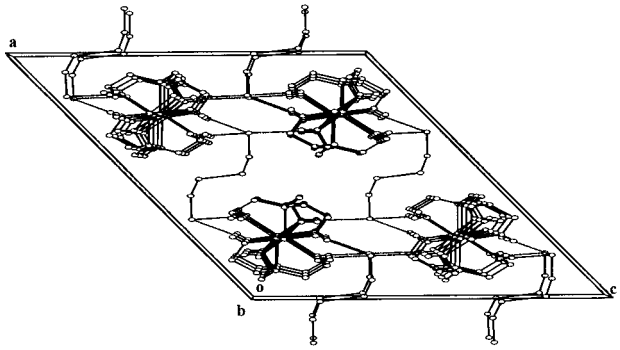

Figure 6. Stereoview of the unit cell showing packing of $\{[NaN(CH_2CH_2OH)_3]_2S_6\}_n$. The a, b, and c axes are oriented as shown.

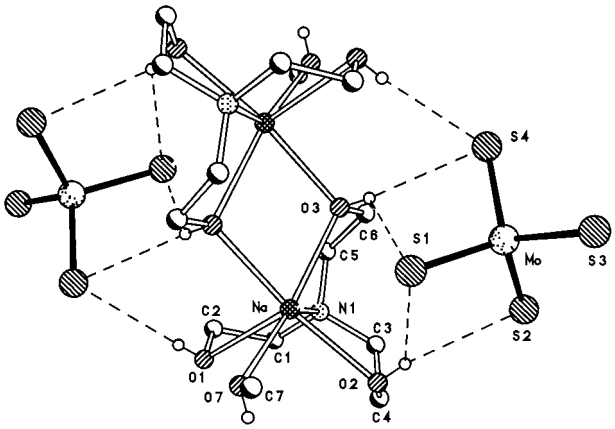

Figure 7. ORTEP diagram of $\{[Na(\mu\text{-}TEA)(CH_3OH)]_2(MoS_4)_2\}^{2-}$. The S···H−O hydrogen bonds are shown in dotted line.

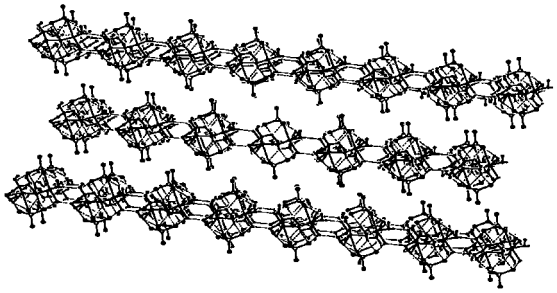

Figure 8. Stereoview of the packing of $\{[Na(\mu\text{-}TEA)(CH_3OH)]_2(MoS_4)_2\}^{2-}$. Parallel one-dimensional extended chains are constructed by hydrogen bonds between the dimer anions.

coordinated CH_3OH molecules in each dimeric structural unit link the CH_2CH_2OH groups of the TEA belonging to neighboring unit by hydrogen bonds, such as O7−H···O1B (2.96 Å). Consequently, a series of parallel one-dimensional extended chains of the dimeric unit make the novel and exquisite structural feature (Figure 8). Selected bond distances and angles are listed in Table 4. The distances of the bonds between Na ion and OH groups can be divided into three types. The shortest Na−O7 (terminal CH_3OH) of 2.378(5) Å and the middle Na−O_{bridge} of 2.434(4)∼2.527(4) Å are comparable to the Na−$O_{terminal}$ and the Na−O_{bridge}, respectively, in complex **3** and other Na/TEA complexes.[2] However, the longest Na−O1 of 2.633(4) Å may occur from the serious distortion of the coordination environment of the Na ion from octahedron. The axis containing Na−O1 and other one O (or N) atom deviates seriously from 180° by 60∼111°. It is also noted that among four Mo−S bond distances three bonds ranging from 2.183(2) Å to 2.191(4) Å are lengthened owing to the S···H−O hydrogen bonding interactions, leaving the shortest Mo−S3 of 2.169(2) Å.

Table 4. Selected Bond Distances (Å) and Angles (deg) for **4**

Mo−S1	2.191(2)	Mo−S2	2.183(2)
Mo−S3	2.169(2)	Mo−S4	2.194(2)
Na−O1	2.633(4)	Na−O2	2.434(4)
Na−O3	2.460(4)	Na−O3A[a]	2.527(4)
Na−O7	2.378(5)	Na−N1	2.553(4)
S1−Mo−S2	109.01(8)	S1−Mo−S3	109.99(8)
S1−Mo−S4	109.91(7)	S2−Mo−S3	110.05(8)
S2−Mo−S4	108.03(8)	S3−Mo−S4	109.82(7)
O1−Na−O2	102.7(1)	O1−Na−O3	121.6(1)
O1−Na−O3A[a]	88.3(1)	O1−Na−O7	77.7(1)
O1−Na−N1	68.9(1)	O2−Na−O3	102.2(1)
O2−Na−O7	88.1(2)	O2−Na−N1	71.9(1)
O3−Na−N1	70.2(1)	O3A[a]−Na−O7	91.4(1)
O3A[a]−Na−N1	115.6(1)	O7−Na−N1	135.4(1)
O3−Na−O3A[a]	73.9(1)	O3−Na−O7	154.4(1)
Na−O3−NaA[a]	106.1(1)	O2−Na−O3A[a]	168.6(1)

[a] Symmetrical operation $1 - x, 2 - y, -z$.

Synthesis of 1−4. Though the reactions of TEA with many metal compounds have been extensively reported, the reaction between TEA and tetrathiometalate has not been reported so far. Compounds **1** and **2** were synthesized in the system containing TEA and tetrathiovanadate in 21% and 17% yields, respectively, and **3** was synthesized in 39% yield. It was reported that VS_4^{3-} hydrolysis takes place in alkali solution, accompanying O/S exchange and the reduction of VS_4^{3-}.[26] Tetrathiovanadate lost all the four sulfur atoms to form the vanadyl/TEA complexes in the reaction with TEA in alkali MeOH solution, indicating the O/S exchange and the reduction from V^V to V^{IV}. It is believed that $V^{IV}O[N(CH_2CH_2O)_2(CH_2CH_2OH)]$ intermediate species, which possess one free arm, may exist in the reaction process and combine each other to form the hexanuclear vanadium crown ether, since V^V/TEA complex with one free CH_2CH_2OH arm has been reported.[15] The structure of the hexanuclear vanadium crown ether contains a μ_3-O_6 cavity suitable to the capture of a Na^+ or Li^+ cation. It is also noted that desulfurization of VS_4^{3-} has been found in other reactions of VS_4^{3-} with bis-salicylaldiminate in MeOH,[26,27] but the place of the sulfur to go in such cases remains to be studied. Complexes **1**−**3** contain a S_6^{2-} group in the molecule indicating where the sulfur has gone in the reaction. Meanwhile, accompanying with the production of the V_6O_6 cluster, the sulfur element in S_8 format has also been separated, implying the self-redox process of VS_4^{3-} to afford V^{4+} and S^0. Compound **3** is a sodium/TEA complex, which was obtained in the reaction system similar to that giving the V_6O_6 cluster. It is considered that the use of $NaNH_2$ instead of NaOMe may increase the activity of Na^+ ion in the reaction with TEA; consequently, compound **3** was separated as major product. It is noted that we cannot isolate the V_6O_6 cluster as pure crystals in the reaction mixture, from which the crystals of **3** were separated, by leaving the solution for prolonged time or concentrating it. It would be a reason that the source of sulfur (VS_4^{3-}) may excessively expend in the production of **3**, causing the difficulty of the isolation for the V_6O_6 cluster that requires S_6^{2-} counterion. We have not yet separated complex **3** or other $[Na(TEA)]_2S_x$ complexes when another source of sulfur, such as $(NH_4)_2S_x$ was used instead of VS_4^{3-}, though the further synthetic research is still in progress. However, it is a pity that we did not clearly know the details of the chemistry in the reaction system. Compound **4** containing the $Na(TEA)^+$ unit was also obtained in the participation of $NaNH_2$, implying the role of the reactant in forming Na/TEA complex. In contrast with the behavior of tetrathiovanadate, tetrathiomolybdate in the reaction with TEA did not desulfurize in comparable conditions, exhibiting the lack of redox reaction. It is also indicated that affinity of molybdenum to sulfur anion is stronger than that of vanadium, restraining the desulfurization of MoS_4^{2-} in the reaction when compared to VS_4^{3-}. Consequently, MoS_4^{2-} does not play the role of the sulfur source to afford S_6^{2-} anion and to cause the formation of complex **3**. Thus MoS_4^{2-} simply joins together with the $[Na(TEA)(MeOH)]^+$ unit by multiple S···H−O hydrogen bonding interactions to form a dimer anion of compound **4**. However, the S···H−O hydrogen bonds together with other hydrogen bonds exist in all the four complexes, giving rise to various structural features and stabilizing these compounds by forming one- or three-dimensional structure.

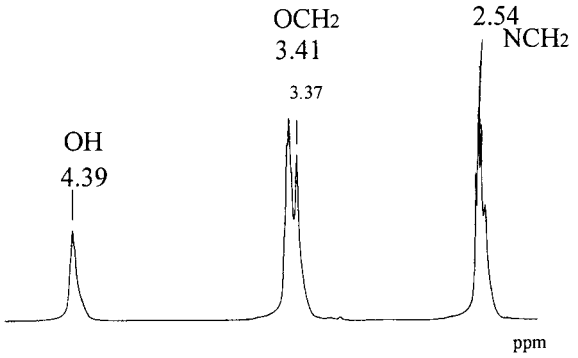

Figure 9. The ^1H NMR spectrum of **3**.

Properties and Spectra. For all the four complexes, the vibrations related to TEA show common feature: O−H at 3154−3390 cm^{-1}, C−O at 1065−1090 cm^{-1}, C−N at 1446−1469 cm^{-1}. Compounds **1** and **2** are green prismy crystals and insoluble in various inorganic and organic solvents. Both the compounds show their spectroscopic features very similarly. The vibrations of OH group were observed at 3382 and 3390 cm^{-1} for **1** and **2**, respectively, showing the existence of the free $HOCH_2CH_2$ arms, and strong absorption peaks at 958 and 949 cm^{-1} are assigned to the V═O stretch.[28] The absorption peaks at 544, 548, and 545 cm^{-1} are assigned to the S−S vibrations of S_6^{2-} anion for **1**, **2**, and **3**. Complex **4** containing MoS_4^{2-} moiety shows a broad peak at 468 cm^{-1} assigned to the Mo═S stretch. The widening and slight red-shift of the signal in comparison with that (472 cm^{-1}) of $(NH_4)_2MoS_4$ [24] are considered to be the influence of the S···H−O hydrogen bonds.

The ^1H NMR spectra were recorded in DMSO-d_6 for the four complexes. Figures 9 and 10 show the ^1H NMR spectra of **3** and **4**, respectively. As expected, the ^1H NMR spectrum of complex **3** is almost consistent to that[29] of free TEA and so are the ^{13}C NMR signals (DMSO-d_6, δ 57.47, 59.54 ppm).[29] These spectra are also close to those of other metal TEA complexes.[2b,3a] Except for the signals from Et_4N^+, the ^1H NMR spectrum of **4** is composed of three sets of signals at 4.81 (−OH), 3.69 ($-OCH_2$), and 2.76 ($-NCH_2$) ppm. In comparison with those of free TEA, the three sets of signals move slightly to downfield. We consider that this may be an indication for the presence[17]

(26) Müller, A.; Krickemeyer, E.; Penk, M.; Walbag, H. J.; Bögge, H. *Angew. Chem., Int. Ed. Engl.* **1987**, *26*, 1045.

(27) (a) Riley, P. E.; Pecoraro, V. L.; Carrano, C. J.; Bonadies, J. A.; Raymond, K. N. *Inorg. Chem.* **1986**, *25*, 154. (b) Bonadies, J. A.; Buttler, W. M.; Pecoraro, V. L.; Carrano, C. J. *Inorg. Chem.* **1987**, *26*, 1218. (c) Wang, X.; Zhang, X.; Liu, X. *Polyhedron* **1995**, *14*, 293.

(28) (a) Selbin, J. *Coord. Chem. Rev.* **1966**, *1*, 293. (b) Selbin, J. *Chem. Rev.* **1965**, *65*, 153.

(29) ^1H NMR (DMSO-d_6): δ 4.37 (3H, OH), 3.41 (6H, OCH_2), 2.54 (6H, NCH_2). ^{13}C NMR (DMSO-d_6): δ 59.19 (OCH_2), 55.98 (NCH_2).

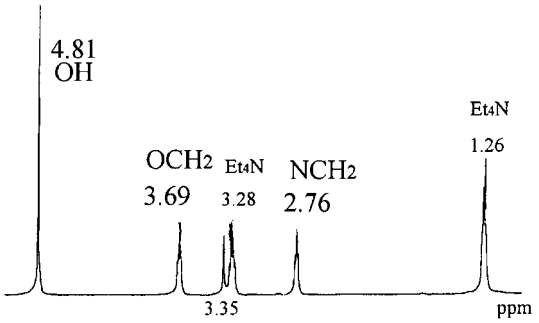

Figure 10. The ^{1}H NMR spectrum of **4**. The signals of TEA ligand slightly shift toward downfield compared to those of free TEA.

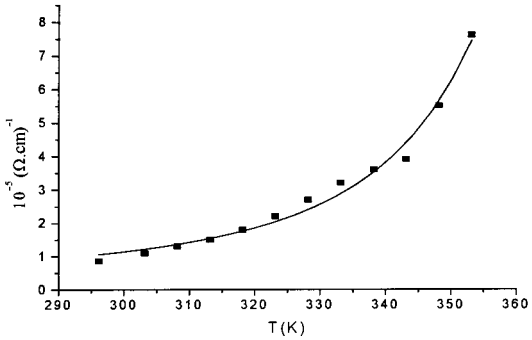

Figure 11. Determined conductance of temperature dependence for **3** in the range from 23 °C to 80 °C.

of weak S···H−O hydrogen bonds in solution for **4**, implying the dimer moiety $\{[(NaTEA)MoS_4]_2\}^{2-}$ remaining in solution. However the ^{1}H NMR spectra for **1** and **2** are difficult to be discussed precisely because of the poor solubility of the two complexes in various solvents. Samples in DMSO-d_6 were almost insoluble and were allowed to stay for several days, consequently only ambiguous broad absorption peaks at 4.14 ppm (OH) and 3.16 ppm (NCH_2) were observed for the two compounds.

A variable-temperature conductance of powdered sample of complex **3** was determined in the range from 23 °C (8.6×10^{-6} $\Omega^{1-}\cdot cm^{-1}$) to 80 °C (7.6×10^{-5} $\Omega^{1-}\cdot cm^{-1}$) as shown in Figure 9. The value of the conductance and its rising tend with the rising of temperature display semiconductor feature of the compound.

Magnetic Property. Compound **1** containing six V^{IV} paramagnetic sites in each of two metal crown ethyl subunits, which connect each other by S_6^{2-} anion. It is believed that the two V_6 subunits are independent and no significant magnetic interaction occurs between them. The magnetic behavior of **1** is studied as the temperature dependence of the effective magnetic moment (μ_{eff}) per V_6 subunit as shown in Figure 11. At 300K, μ_{eff} amounts to 4.04 μ_B, which is close to the value expected for six independent spins $S = {}^1/_2$. When the temperature decreases, the μ_{eff} increases slightly: this behavior is characteristic of a system exhibiting a ferromagnetic interaction. At the lowest temperature recorded, an μ_{eff} value of 6.24 μ_B (5.15 K) is reached, which is slightly below the one expected for a system of spin $S = 3$ ($\mu_{eff} = 6.93$ μ_B). Even neglecting interactions between the two V_6 subunits, the V_6 subunit is still a complicated system. To analyze the magnetic data, an approximation for the V_6 system was made as shown in Scheme 1, in which the V_6 system was divided into two triangular V_3 fragments. Then a molecular field approximation[30] was used to

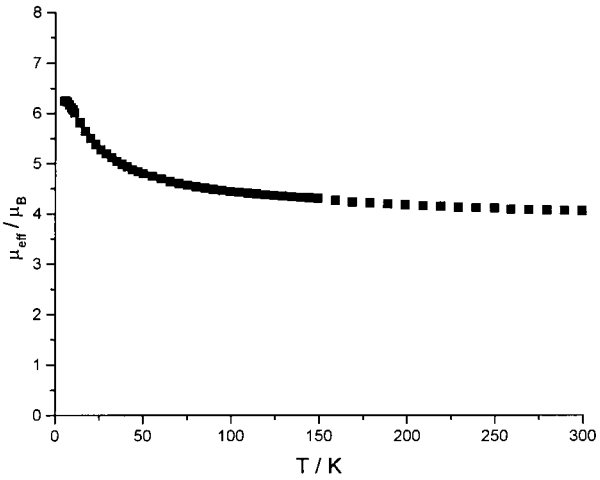

Figure 12. Experimental effect magnetic moment (μ_{eff}) of temperature dependence per V_6 unit in complex **1**.

Scheme 1. A Molecular Field Approximation Model Was Used to Treat the Interaction between the Two V_3 Fragments

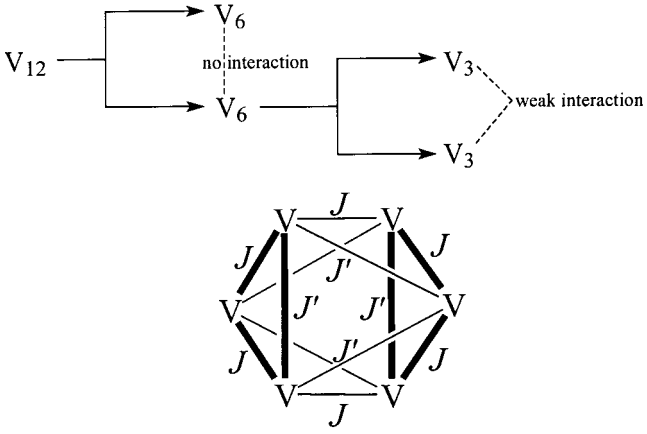

treat the interaction between the two V_3 fragments. Similar approximate approach has been reported[31] previously. Based on Heisenberg-type vector-coupling model, the susceptibilities of the V_3 fragment were obtained from eq 1.

$$\chi_{tri} = \frac{Ng^2\beta^2}{4KT}\left[\frac{10\exp(J/KT) + \exp(-2J/KT) + \exp(-2J'/KT)}{2\exp(J/KT) + \exp(-2J/KT) + \exp(-2J'/KT)}\right] \quad (1)$$

The magnetic interaction between the two V_3 fragments was calculated to get the susceptibilities of the V_6 subunit.

$$\chi = \frac{\chi_{tri}}{1 - [2(J + J')/Ng^2\beta^2]\chi_{tri}} \quad (2)$$

On this basis, the least-squares fitting of the experimental data led to $J = 3.97$ cm^{-1}, $J' = 1.99$ cm^{-1}, and $g = 1.99$, exhibiting that weak ferromagnetic interactions are present in the hexanuclear spin cluster. The agreement factor difined as $F = \sum[(\chi_M)^{calc} - (\chi_M)^{obs}]^2/[(\chi_M)^{obs}]^2$ is equal to 3.64×10^{-3}. Figure 13 shows the fitting curve together with the experimental

(30) O'Connor, C. J. *Prog. Inorg. Chem.* **1982**, *29*, 203.

(31) (a) Handa, M.; Sayama, Y.; Mikuriya, M.; Nukada, R.; Hiromitsu, I.; Kasuga, K. *Bull. Chem. Soc. Jpn.* **1998**, *71*, 119−125. (b) Kou, H.-Z.; Bu, W.-M.; Liao, D.-Z.; Jiang, Z.-H.; Yan, S.-P.; Fan, Y.-G.; Wang, G.-L. *J. Chem. Soc., Dalton Trans.* **1998**, 4161−4164. (c) Shen, H.-Y.; Bu, W.-M.; Gao, E.-Q.; Liao, D.-Z.; Jiang, Z.-H.; Yan, S.-P.; Wang, G.-L. *Inorg. Chem.* **2000**, *39*, 396−400.

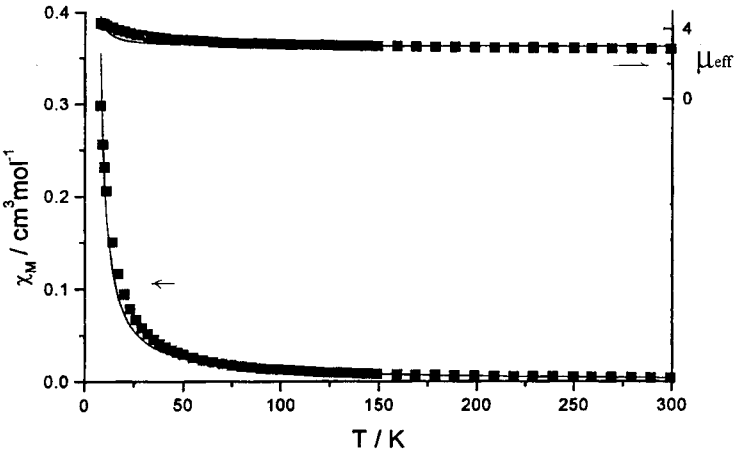

Figure 13. Experimental molar susceptibility (χ_M) and effective magnetic moment (μ_{eff}) of temperature dependence according to each V_3 moiety. The solid line represents the calculated values based on molecular field approximation for the V_3 moiety.

Scheme 2 The Orthogonal Arrangement of d_{xy} Orbitals of Six V^{IV} Sites of syn-Vanadyl Groups May Give Rise to the Ferromagnetic Exchange Interactions

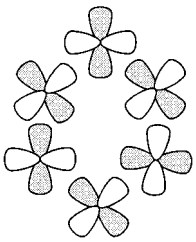

data. However, weak interactions may be attributed to the lack of efficient overlap of the magnetic orbitals, which are considered as d_{xy},[32] because of the cyclic nonplanar structure of the V_6 subunit. It is believed that the magnetic coupling pathways can also be afforded by double μ-O bridging groups. The value and sign of the magnetic interaction between the V^{IV} sites are structurally sensitive, which are decided by the geometry of the vanadyl units such as syn or anti coplanar or twist.[32,33] Most of the literature reported antiferromagnetic interaction of $V^{IV}-V^{IV}$, the J values from negative one to negative numbers in the hundreds cm^{-1}, but there are also some reports about the ferromagnetic interaction[34] transmited by a variety of bridge units. It is considered that the hexanuclear cyclic syn-vanadyl structure may be favorable to the orthogonal arrangement of d_{xy} orbitals (Scheme 2), which gives rise to the ferromagnetic exchange interactions between the V^{IV} sites.

Density Functional Calculation. DFT calculation has been performed for compound **1** and its analogues using the Amsterdam Density Functional package (ADF) developed by Baerends.[35] An uncontracted single-ξ STO basis set has been used for 4s, 4p, and 3d orbitals of V atoms, 2s and 2p of O and C atoms, and 1s of H atoms. The calculations have been performed on the LSD level with the VWN[36] approximation.

The electronic structure and magnetic moment of the $\{M\subset V_6O_6[N(CH_2CH_2O)_2(CH_2CH_2OH)]_6\}$ complexes (M = Li^+, Na^+, K^+, and nothing) were studied by using the methods depicted above. As aforementioned only the structure of the complex with M = Na^+ has been determined in which the sodium ion is captured into a $V_6(\mu_3\text{-O})_6$ cavity. The crystal structures with M = Li^+ and K^+ have not been reported and are considered to be the same as that of complex **1**. So, the structural data of the complex with M = Na^+ are also used in the calculation for the Li^+ and K^+ analogues by replacing the Na^+ with Li^+ and K^+, respectively. The complex with no alkali metal ion enclosed is a supposed complex and the calculation on it is for the sake of evaluating the interaction energy between M and the $V_6O_6[N(CH_2CH_2O)_2(CH_2CH_2OH)]_6$ cluster. To reduce the time and space consumptions, the terminal C_2H_4OH is replaced by H and this simplification is expected to not affect the structure of the center $V_6(\mu_3\text{-O})_6$ backbone. The calculated results for M = Li^+, Na^+, K^+, and nothing, respectively, are summarized in Tables 5 and 6. Among all the complexes with obvious number (6, 4, and 2) of the unpaired electrons, the structures with six unpaired electrons are a little more stable than those with 2 and 4 unpaired electrons, indicating the stability of a V_6 system with six independent spins $S = {}^1/_2$. The effect magnetic moment of complex **1** containing the $[Na\subset V_6(\mu_3\text{-O})_6]$ backbone has been determined to be consistent with the value expected to the system with six $S = {}^1/_2$ spins. From the configuration of the M ion it is obvious that the magnetic moment of the M ion enclosed in the $V_6(\mu_3\text{-O})_6$ backbone is close to zero, meaning that the unpaired electrons all come from V ions. The M ion does not affect significantly the configuration of the V ions. The main components of the HOMO and LUMO are the orbitals of the unpaired electrons. The stabilization energies (E_b) were listed in Table 5 when

Table 5. The Total Bonding Energy, HOMO, LUMO, and the Binding Interaction (E_b) between M and $[V_6(\mu_3\text{-O})_6]$

$[M\subset V_6(\mu_3-O)_6]$	unpaired electron	bond energy (eV)	HOMO (a.u.)	LUMO (a.u.)	E_b (eV)
M = Li^+	6	−871.711	−0.0028	0.0333	12.98
M = Li^+	4	−870.924	0.0146	0.0149	
M = Li^+	2	−871.701	−0.0028	0.0343	
M = Na^+	6	−874.001	−0.0014	0.0401	12.92
M = Na^+	4	−873.222	0.0196	0.0204	
M = Na^+	2	−873.991	−0.0025	0.0401	
M = K^+	6	−868.379	−0.0010	0.0399	7.491
M = K^+	4	−867.558	0.0164	0.0172	
M = K^+	2	−868.368	−0.0021	0.0399	
M = nothing	6	−863.510	0.1162	0.1474	
M = nothing	4	−862.753	0.1301	0.1308	
M = nothing	2	−863.504	0.1130	0.1478	

(32) Dean, N. S.; Bond, M. R.; O'Connor, C. J.; Carrano, C. J.; Zubieta, J. *Inorg. Chem.* **1996**, *35*, 7643.
(33) Plass, W. *Angew. Chem., Int. Ed. Engl.* **1996**, *35*, 627.
(34) (a) Darkwa, J.; Lockemeyer, J. R.; Royd, P. D. W.; Rauchfuss, T. B.; Rheingold, A. L. *J. Am. Chem. Soc.* **1988**, *110*, 141. (b) Bond, M. R.; Mokry, L. M.; Otieno, T.; Thompson, J.; Carrano, C. J. *Inorg. Chem.* **1995**, *34*, 1894. (c) Getteschi, D.; Tsukerblutt, B.; Barra, A. L.; Brunel, L. C.; Müller, A.; Döring, J. *Inorg. Chem.* **1993**, *32*, 2114.
(35) *ADF 1.15*; Department of Theoretical Chemistry, Vrije Universteit: Amsterdam, 1995.
(36) Vosko, S. H.; Wilk, L.; Nusair, M. *Can. J. Phys.* **1980**, *58*, 1200.

Table 6. The Electronic Configuration of M and V in the $[M\subset V_6(\mu_3\text{-}O)_6]$ Cluster

$[M\subset V_6(\mu_3-O)_6]$	unpaired electron	M[a]	V (α electrons)	V (β electrons)
$M = Li^+$	6	$s^{0.43}p^{0.88}$	$d^{1.98}s^{0.27}p^{0.54} \times 6$[b]	$d^{0.93}s^{0.25}p^{0.51} \times 6$
$M = Li^+$	4	$s^{0.44}p^{0.87}$	$d^{1.98}S^{0.27}p^{0.53} \times 4$	$d^{0.93}s^{0.25}p^{0.51} \times 4$
			$d^{1.45}S^{0.26}p^{0.53} \times 2$	$d^{1.44}s^{0.26}p^{0.53} \times 2$
$M = Li^+$	2	$s^{0.44}p^{0.88}$	$d^{1.98}s^{0.27}p^{0.54} \times 4$	$d^{1.97}s^{0.27}p^{0.54} \times 2$
			$d^{0.93}s^{0.26}p^{0.51} \times 2$	$d^{0.93}s^{0.26}p^{0.51} \times 4$
$M = Na^+$	6	$s^{0.22}p^{0.26}$	$d^{1.99}s^{0.27}p^{0.55} \times 6$	$d^{0.92}s^{0.27}p^{0.53} \times 6$
$M = Na^+$	4	$s^{0.22}p^{0.25}$	$d^{1.99}s^{0.27}p^{0.55} \times 4$	$d^{0.99}s^{0.27}p^{0.55} \times 4$
			$d^{1.45}s^{0.27}p^{0.54} \times 2$	$d^{1.45}s^{0.27}p^{0.54} \times 2$
$M = Na^+$	2	$s^{0.22}p^{0.26}$	$d^{1.98}s^{0.27}p^{0.55} \times 4$	$d^{1.98}s^{0.27}p^{0.55} \times 2$
			$d^{0.94}s^{0.26}p^{0.52} \times 2$	$d^{0.94}s^{0.26}p^{0.52} \times 4$
$M = K^+$	6	$s^{0.36}p^{0.48}$	$d^{1.98}s^{0.27}p^{0.54} \times 6$	$d^{0.92}s^{0.26}p^{0.52} \times 6$
$M = K^+$	4	$s^{0.36}p^{0.48}$	$d^{1.98}s^{0.27}p^{0.55} \times 4$	$d^{0.93}s^{0.26}p^{0.52} \times 4$
			$d^{1.45}s^{0.27}p^{0.53} \times 2$	$d^{1.44}s^{0.27}p^{0.53} \times 2$
$M = K^+$	2	$s^{0.36}p^{0.48}$	$d^{1.98}s^{0.27}p^{0.55} \times 4$	$d^{1.98}s^{0.27}p^{0.54} \times 2$
			$d^{0.93}s^{0.26}p^{0.52} \times 2$	$d^{0.92}s^{0.26}p^{0.52} \times 4$
M = nothing	6		$d^{1.96}s^{0.27}p^{0.56} \times 6$	$d^{0.93}s^{0.26}p^{0.53} \times 6$
M = nothing	4		$d^{1.96}s^{0.27}p^{0.55} \times 4$	$d^{0.92}s^{0.26}p^{0.53} \times 4$
			$d^{1.45}s^{0.27}p^{0.55} \times 2$	$d^{1.43}s^{0.27}p^{0.55} \times 2$
M = nothing	2		$d^{1.96}s^{0.27}p^{0.56} \times 4$	$d^{1.96}s^{0.27}p^{0.56} \times 2$
			$d^{0.94}s^{0.26}p^{0.53} \times 2$	$d^{0.93}s^{0.26}p^{0.53} \times 4$

[a] For M, in all cases the alpha configuration is equal to the beta configuration. [b] All the symbols "$\times$ *n*" in this table mean that there are *n* atoms having the configuration.

inserting the M ion into the $[V_6(\mu_3\text{-}O)_6]$ hole. All the positive values were obtained for Li^+, Na^+, and K^+, meaning that the insertion of the alkali metal ion depresses the total energy and thus these complexes may exist. It is worthwhile to notice that the E_b values for Li^+ and Na^+ are almost the same, but much larger than that of K^+, implying the less stability of $[K\subset V_6(\mu_3\text{-}O)_6]$ complex than that of Na^+ and Li^+ analogues. The net charge of Li in $[Li\subset V_6(\mu_3\text{-}O)_6]$ is negative. The bonding interaction between Li and adjacent O is believed to be both covalent and ionic. Consequently, the net negative charge should come from the adjacent O donors coordinated to Li. In contrast to $[Li\subset V_6(\mu_3\text{-}O)_6]$, $[K\subset V_6(\mu_3\text{-}O)_6]$ and $[Na\subset V_6(\mu_3\text{-}O)_6]$ have a net positive charge on the respective alkali metal atom enclosed in the $V_6(\mu_3\text{-}O)_6$ backbone, meaning the interaction between K (or Na) and the adjacent O donors is mostly ionic. Though the central cavity of the $V_6(\mu_3\text{-}O)_6$ with the diameter of 4.69 Å (the distance between opposite μ_3-O atoms) seems too small to insert the K^+ ion since the sum of the ionic radii ($r_{K^+} + r_{O^{2-}} = 2.68$ Å) is larger than the hole size, the hole may be enlarged to capture the K^+. Another prominent example, $[K\subset(VO)_4(\mu\text{-}O)_3(\mu\text{-}OH)(\mu\text{-}O_2CR)_4]$,[37] for an inorganic crown ether analogue has been reported, although, in this case the cavity is even smaller. However, the even lower stabilization energy (E_b) indicates the K^+ complex to be less stable than the Na^+ complex, though the K^+ can also be expected to insert into the $V_6(\mu_3\text{-}O)_6$ center hole. This should be a reason we have not yet got the complex with $M = K^+$. As a result, the large E_b of $[Li\subset V_6(\mu_3\text{-}O)_6]$ is so because of the coordination stabilization, while the large E_b of $[Na\subset V_6(\mu_3\text{-}O)_6]$ is so because of both the space suitability ($r_{Na^+} + r_{O^{2-}} = 2.33$ Å) and the bonding interaction.

Acknowledgment. This work was supported by State Key Basic Research and Development Plan of China (G1998010100) and NNSFC (No. 29733090, No. 29973047, and No. 39970177).

Supporting Information Available: Tables of crystallographic data, atomic coordinates and *B* values, bond lengths and angles, and anisotropic thermal parameters for complexes **1**, **3**, and **4**. This material is available free of charge via the Internet at http://pubs.acs.org.

IC010126C

(37) Rehder, D. *Mol. Eng*. **1993**, *3*, 121.